Desalination and Water Treatment
www.deswater.com
doi: 10.1080/19443994.2013.809638

52 (2014) 1725–1734
February

Taylor & Francis
Taylor & Francis Group

Simulation of an autonomous solar vacuum membrane distillation for seawater desalination

Nader Frikha[a,*], Radhouane Matlaya[b], Béchir Chaouachi[b], Slimane Gabsi[c]

[a]*Higher Institute of Biotechnology, Sfax University, Street Soukra BP 261, 3038 Sfax, Tunisia*
Fax: +216 7539 2190; email: naderfrikha@yahoo.fr
[b]*National School of Engineers of Gabes, Gabes University, Street Omar Ibn ElKhattab, Gabes 6029, Tunisia*
[c]*National School of Engineers of Sfax, Sfax University, Street Omar Ibn ElKhattab, Sfax 6029, Tunisia*

Received 9 December 2011; Accepted 20 April 2013

ABSTRACT

Several papers deal with membrane distillation of seawater and mainly focus on the choice of membranes and comparison of this technique with other desalination techniques, but there are very few studies that quantitatively estimate the potential of this technology coupled with solar energy. The objective of this work is to develop a model describing the operation of a desalination membrane powered by solar energy. This model determines the performance of the unit over time and for any day of the year. This model is established from the balance equations of mass and heat on the different units (membrane, exchanger, condenser, and field of solar collectors). The model is used to evaluate the evolution of the distillate flow rate and temperature changes for different flows. The model also allows to estimate the productivity of the unit during the year. The simulation of the operation of the unit shows that the daily production of distilled water is between 63 and 188 kg/m^2 for the days of 21 December and 21 June.

Keywords: Membrane distillation; Solar collectors; Photovoltaic cells

1. Introduction

Tunisia is located on the southern rim of the Mediterranean basin. Like its neighbor countries, it is confronted by a problem of fresh water shortage [1]. In fact, it has very limited water resources and has a high degree of salinity, aggravated by a large spatial and temporal disparity between southern and northern parts, and fluctuations from one year to another [2].

Tunisia has mobilized a large proportion of its water resources (surface and underground waters) using dams, transport aqueducts, small lakes, deep wells, and desalination plants. For big cities and large-scale agglomeration, the problem of fresh water is currently resolved. In remote rural communities, the problem of drinking water remains unresolved.

Desalination using solar energy coupled with membrane technology is considered an attractive alternative to the production of drinking water especially in rural and arid areas. On the other hand, Tunisia offers great

*Corresponding author.

Presented at the Third Maghreb Conference on Desalination and Water Treatment (CMTDE 2011) Hammamet, Tunisia, 18–22 December 2011

opportunities for the development of solar applications through the exploitation of solar energy. And because of its geographical location, Tunisia has one of the highest solar radiations in the world [3].

The crisis of drinking water announced for the coming years raises the interest of rapid development of desalination technologies cheaper, simpler, more robust, more reliable, and less energy intensive and environmentally friendly. In this context and as part of the European project MEDINA (Membrane-Based Desalination: An Integrated Approach, Project No: 036997), we have designed and realized a membrane distillation (MD) unit coupled with solar energy. The installation is completely autonomous; indeed, the only energy source is the sun. The electrical energy required to operate the plant is produced by means of a field of photovoltaic cells with a peak power of 2.1 kW. The heating of seawater is provided by a field of flat solar collectors with a total area of 70 m^2.

MD is a hybrid of thermal distillation and membrane processes. This process employs a hydrophobic microporous membrane to support a vapor–liquid interface. Generally, the transport mechanism of MD can be summarized in the following steps:

- Evaporation of water at the warm feed side of the membrane.
- Migration of water vapor through the nonwetted pores.
- Condensation of water vapor transported at the permeate side of the membrane.

Regarding the vacuum membrane distillation (VMD), the vapor is withdrawn by applying a vacuum on the permeate side. The permeate-side pressure is lower than the saturation pressure of the evaporating species and the condensation of the permeate takes place outside the module. The diffusion of the vapor through the membrane pores is made according to a Knudsen mechanism [4,5]. Permeate condensation takes place outside the module, inside a condenser, or a trap containing liquid nitrogen.

The MD technique holds important advantages with regard to the implementation of solar-driven stand-alone operating desalination systems [6–8]. The most important advantages are:

- The operating temperature of the MD process is in the range of 60–80 °C. This is a temperature level at which thermal solar collectors perform well.
- Chemical feed water pretreatment is not necessary.
- Intermittent operation of the module is possible.
- Contrary to RO, no damage occurs if membranes dry out [9].
- System efficiency and high product water quality are almost independent from the salinity of the feed water.

2. Principle of functioning

The choice of unit design and dimensions of its components is the result of work carried out in the project MEDINA. These studies allowed to compare the performance of different configurations (membrane module integrated within the absorber, module separated from the solar collector …) and to design the various organs of the plant chosen [10,11].

The unit was installed in the village of orphaned children (SOS MAHRES). This is a set of houses located close to the city of Mahres in the region of Sfax. This is a nongovernmental social, care, and foster care of children without family support. It was created in 1949 to improve the living conditions of children in distress. There are currently 13 family houses, a playground, a kids club, shops and services, and domestic appliances. The capacity is 104 children: 8 children per family home.

Fig. 1 shows the desalination plant and various instrumentation and control regulation.

The main components of desalination plant are:

- A membrane module: (UMP 3247 R) with 806 fibers (PVDF) with an internal diameter of 1.4 mm. This module has a length of 1.129 m and offers a total area of 4 m^2.
- Field of solar collector (seven rows and five collectors in series, total area: 70 m^2).
- Field of solar photovoltaic modules (16 modules, peak power: 2.1 kW).

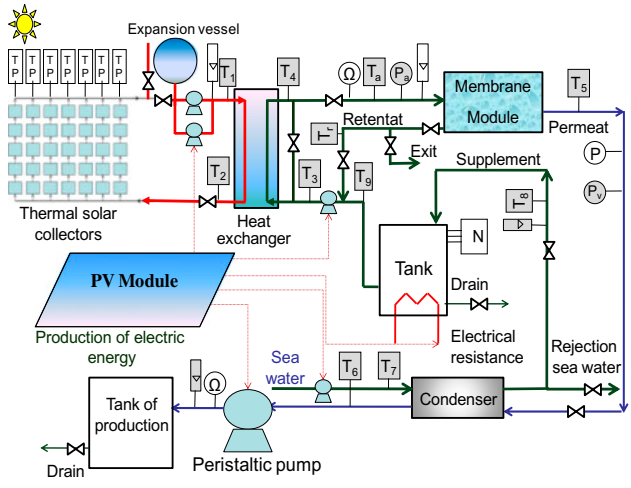

Fig. 1. Design of the solar VMD desalination plant.

- Flow pump ensuring the supply of seawater (Flow up to 2,500 l/h, power: 1 kW).
- Circulator pump circulates the coolant in the collector field (power: 0.5 kW).
- Peristaltic pump used for the recovery the distillate product (power: 0.5 kW).
- Plate heat exchanger with 27 titanium plates and offering an exchange area of 1.08 m^2 (maximal power of heat exchange: 26 kW).
- Condenser used for the condensation of the steam produced.
- Instrumentation and control regulation.
- Mixing tank (volume: 80 L).
- Tank of fresh water production (volume: 2 m^3).

In the proposed flow sheet (Fig. 1), the coolant fluid out of the field of solar collectors is routed to the heat exchanger to provide heat to the seawater at the inlet of membrane module.

The temperature of seawater at the outlet of the heat exchanger should not exceed 75°C for the structure of membranes cannot resist high temperatures that can cause an alteration of their mechanical strength.

The salinity of the supply of the membrane is controlled by a conductivity meter placed at the inlet of the membrane module. The salinity must not exceed a maximum permitted level in order to limit membrane fouling. If the maximum level of salinity is not exceeded, retentate exiting the membrane module is sent to the exchanger and is mixed with an addition of preheated seawater. If the maximum level is exceeded, the retentate will be rejected and retenate feeding the membrane module is made from the mixing tank.

The amount of vapor produced supplies the condenser. After condensation, a peristaltic pump mounted downstream of the condenser ensures the delivery of production of desalinated water. The condensation of vapor produced preheats the flow of seawater supplementary. A level switch installed on the tank controls the flow of seawater supplementary through a solenoid valve. The flow of seawater to the input of the condenser is of the order of 3,000 l/h.

3. Modeling

With the aim to simulate the operation of the unit, a model describing the functioning of the components, including the solar collector, heat exchanger plate, and the membrane module unit, has been developed.

3.1. Dynamic modeling of the solar collector

The most important element in the solar collector is the absorber plate. The energy release is captured by passing a heat transfer fluid in a tube in contact with the metal surface (Fig. 2).

The solar radiation reaches the absorber after passing through the glass. This incident solar energy absorbed is not entirely transmitted to the fluid, because a part of it is dissipated as heat loss from the absorber and the glass, on the one hand, and the glass and the ambient medium on the other.

It is assumed that the flow is divided equally into seven cascades, each with five collectors and the temperature at the output of a collector is the same as at the entrance to his successor without considering losses in the conduits.

The two-temperature model was adopted. This model considers that the temperature of the absorber and the fluid are different at every point, it is assumed that the fluid velocity is uniform [12].

The energy balance on the absorber and the coolant flowing through the tube in contact with the absorbing surface leads to the following system of equations.

3.1.1. Absorber

$$\begin{cases} q_{\text{accumulated,Ab}} = q_{\text{absorbed}} - q_{\text{lost}} - q_{\text{used}} \\ \rho_{\text{Ab}} dV_{\text{Ab}}\, Cp_{\text{Ab}} \frac{\partial T_{\text{Ab}}(z,t)}{\partial t} = \alpha\tau E(t) l_{\text{Ab}} dz - Ul_{\text{Ab}} dz (T_{\text{Ab}} - T_{\text{amb}}) \\ \qquad\qquad - h_{\text{Fd}} dS (T_{\text{Ab}} - T_{\text{Fd}}) \end{cases} \tag{1}$$

3.1.2. Coolant

$$\begin{cases} q_{\text{accumulated,Fd}} = q_{\text{input}} - q_{\text{output}} + q_{\text{used}} \\ \rho_{\text{Fd}} dV_{\text{Fd}}\, Cp_{\text{Fd}} \frac{\partial T_{\text{Fd}}(z,t)}{\partial t} = Q_{\text{v}} \rho_{\text{Fd}} Cp_{\text{Fd}} (T_{\text{Fd}}(z,t) - T_{ref}) \\ -Q_{\text{v}} \rho_{\text{Fd}} Cp_{\text{Fd}} (T_{\text{Fd}}(z+dz,t) - T_{\text{ref}}) + h_{\text{Fd}} dS (T_{\text{Ab}} - T_{\text{Fd}}) \end{cases} \tag{2}$$

q_{used}: heat flow exchanged by convection between the absorber plate and the fluid.
dV_{Ab}: elementary volume of the absorber

$$dV_{\text{Ab}} = S_{\text{Ab}}\, dz \tag{3}$$

dV_{Fd}: elementary volume of the coolant

$$dV_{\text{Fd}} = S_{\text{tube,int}}\, dz \tag{4}$$

S_{Ab}: area of heat accumulation

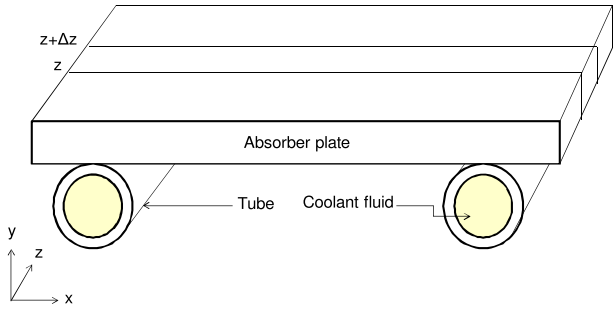

Fig. 2. Schema of the absorber.

$$S_{Ab} = \frac{\pi}{4}\left(d_{ex}^2 - d_{in}^2\right) + l_{Ab}e \tag{5}$$

$S_{tube,int}$: tube inner area

$$S_{tube,int} = \frac{\pi}{4}d_{in}^2 \tag{6}$$

dS: elementary surface of the absorber

$$dS = \pi\, d_{in}\, dz \tag{7}$$

Q_v: flow rate flowing through a tube

$$Q_v = S_{tube,int} v_{Fd} \tag{8}$$

Finally, relations 1 and 2 can be rewritten as:

$$\begin{cases} \dfrac{\partial T_{Ab}(z,t)}{\partial t} = \dfrac{1}{\rho_{Ab} S_{Ab}\, Cp_{Ab}}\left[h_{Fd}\pi d_{in}(T_{Fd} - T_{Ab}) + Ul_{Ab}(f(t) - T_{Ab})\right] & (9) \\ \dfrac{\partial T_{Fd}(z,t)}{\partial t} = v_{Fd}\dfrac{\partial T_{Fd}(z,t)}{\partial z} + \dfrac{h_{Fd}}{\rho_{Fd}\, Cp_{Fd}\frac{d_{in}}{4}}(T_{Ab} - T_{Fd}) & (10) \end{cases}$$

where $f(t)$represents the function : $f(t) = \dfrac{\alpha\tau E(t)}{U} + T_{amb}$ (11)

This model will determine the temperature of the coolant at the exit of solar collector.

3.2. Dynamic modeling of the plate heat exchanger

An energy balance under transient conditions for each fluid is established. The terms of conduction in the fluid, the work of pressure forces, and viscous dissipation effects are neglected. In our case, it is necessary to solve a system of equations describing the evolution of the temperature in the compartments between the 27 plates of the exchanger as well as the plates themselves.

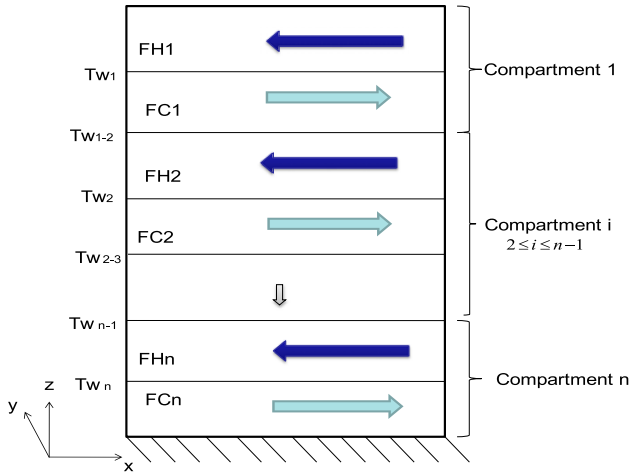

Fig. 3. Simplified scheme of the heat exchanger. FH_i: hot fluid flowing through a compartment i. FC_i: cold fluid flowing through a compartment i. Tw_i,$Tw_{i,i+1}$: wall temperature in the same block and wall temperature between two successive blocks.

Fig. 3 helps to clarify this provision. The difficulty of solving the problem is particularly thermal coupling between the two fluids. In addition, there are no boundary conditions on both sides of the plate; we have just the inlet temperatures of the two fluids that vary over time depending on the solar flux.

The problem comes down to writing the balances in n compartments. The energy balance applied to the different compartments is given by:

$$\begin{aligned} \text{Hot fluid} : (\rho_{Fd} dVCp)_{Hi}\frac{dT_{Hi}}{dt} &= \dot{m}_{Hi} Cp_{Hi}\left(-\frac{dT_{Hi}}{dx}\right) - h_{Hi} dS(T_{wi} - T_{Hi}) \\ &\quad - h_{Hi} dS(T_{p\,i-1,i} - T_{Hi}) \end{aligned} \tag{12}$$

For the first compartment ($i = 1$), energy exchange between the top wall and the fluid is zero.

$$\text{Cold fluid} : (\rho dVCp)_{Ci}\frac{dT_{Ci}}{dt} = \dot{m}_{Ci}Cp_{Ci}\left(-\frac{dT_{Ci}}{dx}\right) - h_{Ci}dS(T_{Ci} - T_{wi}) - h_{Ci}dS(T_{Ci} - T_{wi,i+1})$$

For the last compartment ($i = n$), the exchange of energy between bottom wall and the fluid is zero.With ρ_{Fd}, the density of the fluid and h_C and h_F are, respectively, the exchange coefficients side cold fluid and hot fluid side.

For a plate separating the two fluids in the same compartment (Tp_i):

$$(\rho_{plate}dVCp_{plate})_i\frac{dT_{wi}}{dt} = h_{Ci}dS(T_{Ci} - T_{wi}) - h_{Hi}dS(T_{wi} - T_{Hi}) \quad (14)$$

For a plate between two compartment $Tp_{i,i+1}$:

$$(\rho_{plate}dVCp_{plate})_{i,i+1}\frac{dT_{wi,i+1}}{dt} = h_{Hi+1}dS(T_{wi,i+1} - T_{Hi+1}) - h_{Ci}dS(T_{Ci} - T_{wi,i+1}) \quad (15)$$

Thus our case, the exchanger consists of 27 plates ($m = 27$) corresponding to 14 compartments ($n = (m + 1)/2 = 14$). The resulting model has 55 equations ($4n - 1$).

3.3. Dynamic modeling of hollow fiber membrane

To establish a model that determinates the temperature of the retentate and the vapor produced and the flow of permeate and retentate, we propose to perform a heat and matter balance on an elementary volume dV. For a given fiber, when the feed liquid flows through the elementary volume dV, a quantity of water evaporates and thus the flow of water to be treated decreases and the water temperature varies. So, there is a simultaneous transfer of mass and heat. The module configuration studied is internal–external: the feed fluid flows inside the fibers. Depression is applied to the outside of the fibers and the permeate flow is directed from inside the fibers out. Fig. 4 illustrates an element of volume in the fiber membrane module.

For the calculation of energy balance, the following assumptions were taken into account:

- The radial propagation of heat is negligible and, therefore, all fibers will be at the same temperature for the same side z.

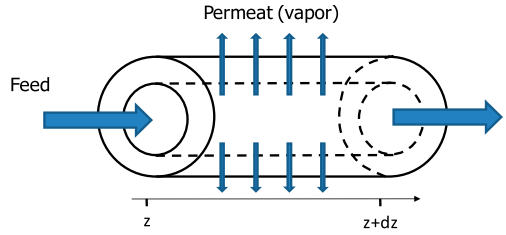

Fig. 4. Volume element of a hollow fiber.

- The transfer of water molecules in the gas phase through the pores of the membrane by the Knudsen diffusion mechanism [13,14].
- The coefficient of permeability of the membrane k_m (Knudsen permeability) is a function of temperature at the interface of the membrane (Ti) and can be expressed as follows [15]:

$$k_m = k_{m0}\,T_i^{0,5} \quad (16)$$

- The saturated vapor pressure P_s can be expressed using the equation of Antoine [16]. P_s is in Pa and the temperature T_z is in Kelvin.

$$P_s = \exp\left(A_1 - \frac{A_2}{T_z - A_3}\right) \text{ with } A_1 = 23.1964 \quad A_2 = 3816.44 \quad A_3 = 46.13 \quad (17)$$

The flux density of water vapor through the internal interface membrane-water ($kg\,s^{-1}\,m^{-2}$) is described by the following equation:

$$J_v = k_m[P_s - P_{vacuum}] \quad (18)$$

The balance under transient conditions applied to a fiber in a volume element dV can be written as follows:

$$\dot{m}_{feed,z}Cp_l(T_z - T_{ref}) = \dot{m}_{feed,z+dz}Cp_l(T_{z+dz} - T_{ref}) + (\dot{m}_{feed,z} - \dot{m}_{feed,z+dz})L_v + \rho_l dVCp_l\frac{d(T_z - T_{ref})}{dt} \quad (19)$$

By performing a mass balance, the distillate flow rate produced between z and $z + dz$ is:

$$d\dot{m}_{dist} = J_v\,dS = J_v\,(n_{fib}\,\pi\,d_{fib}\,dz) \quad (20)$$

Given that $d\dot{m}_{dist,z} = -d\dot{m}_{feed,z}$ we can write:

$$\frac{d\dot{m}_{\text{feed}}}{dz} = -n_{\text{fib}}\,\pi\,d_{\text{fib}}\,J_{\text{v}} \tag{21}$$

$$\text{With } J_{\text{v}} = k_{\text{m0}}\,T_z^{-0.5}\left[\exp\left(A_1 - \frac{A_2}{T_z - A_3}\right) - P_{\text{vacuum}}\right] \tag{22}$$

With n_{fib} is the number of fibers, d_{fib} is the diameter of a fiber, dz is the element of length, and dS is the elementary surface of the membrane relative to the volume dV.

By combining the two balance equations, the final equation describing the evolution of the temperature of the retentate over time and space is obtained:

$$\frac{dT_z}{dt} = -v_{\text{feed}}\frac{dT_z}{dz} - \frac{4J_{\text{v}}}{\rho_l\,d_{\text{fib}}Cp_l}[Cp_l(T_{\text{ref}} - T_z) + L_v] \tag{23}$$

v_{feed} represents the velocity of seawater:

$$v_{\text{feed}} = \frac{\dot{m}_{\text{feed}}}{\rho_l\left(n_{\text{fib}}\frac{\pi d_{\text{fib}}^2}{4}\right)} \tag{24}$$

Solving the differential equation will determine the amount of distillate produced and the temperature of the liquid to each element of fiber length and thus the temperature at the exit of the membrane module.

$$\dot{m}_{\text{d}} = \int_0^L n_{\text{fib}}\,\pi\,d_{\text{fib}}k_{\text{m0}}\,T_z^{-0,5}\left[\exp\left(A_1 - \frac{A_2}{T_z - A_3}\right) - P_{\text{vacuum}}\right]dz \tag{25}$$

3.4. Resolution method

There are several ways to solve a system of partial differential equations nonlinear. In our case, the regressive method of finite differences was used. The method consists in discrediting the equations in order to have a matrix that contains the terms of the system. This matrix is solved by the iterative method of Gauss Seidel. Three simulation programs were developed on the calculation software MATLAB.

4. Experimental validation and model runs

The models developed describe the operation of the collector field, the plate heat exchanger, and the membrane module. The results mainly concern the variation of different temperatures over time and space, and the daily production of distillate.

4.1. Experimental validation

The experimental validation is an essential step for evaluating the performance of the model and its exploitation. To test the validity and quantify variation between model and experiment, we calculated the average error and the mean temperature difference, why we used the following two equations:

$$\text{Average error : } \text{Er}_{\text{average}} = \frac{1}{n_t}\sum_{i=1}^{n_t}\frac{|T_{\text{exp},i} - T_{\text{mod},i}|}{T_{\text{exp},i}} \tag{26}$$

Average temperature difference :

$$\overline{\Delta T} = \frac{1}{n_t}\sum_{i=1}^{n_t}|T_{\text{exp},i} - T_{\text{mod},i}| \tag{27}$$

The comparison between the experimental temperature profiles and those obtained by simulation for several days shows that the three established models describe well the experiment. In effect, the calculated deviation of the tests performed on the heat exchanger does not exceed 8.2% and the average difference in temperature is 4°C.

As an example, Figs. 5 and 6 present a comparison of model results (fields of solar collectors and heat exchanger) and the experimental results:

The temperature profiles of the coolant and the feed water are relatively smooth. These temperatures depend only on the measured solar flux, the feed flow rate, and the coolant flow rate. These flow rates are maintained constant and the 9 June was a sunny day (the solar flux was regular).

It is noted that the temperature of the seawater at the outlet of the heat exchanger is close to the maximum allowable temperature of the membrane (75°C).

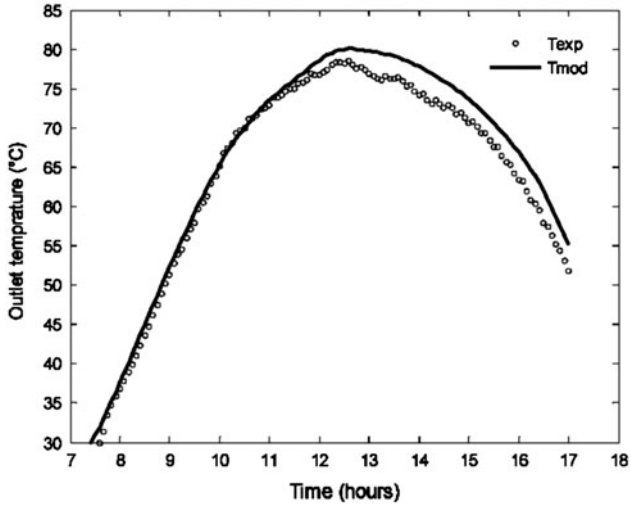

Fig. 5. Comparison of experimental and calculated temperatures at the outlet of the solar collector fields. Day: 9 June 2011, flow of coolant $\dot{m}_{\text{coolant}} = 770$ kg/h, flow of cold fluid $\dot{m}_{\text{feed}} = 1{,}200$ kg/h.

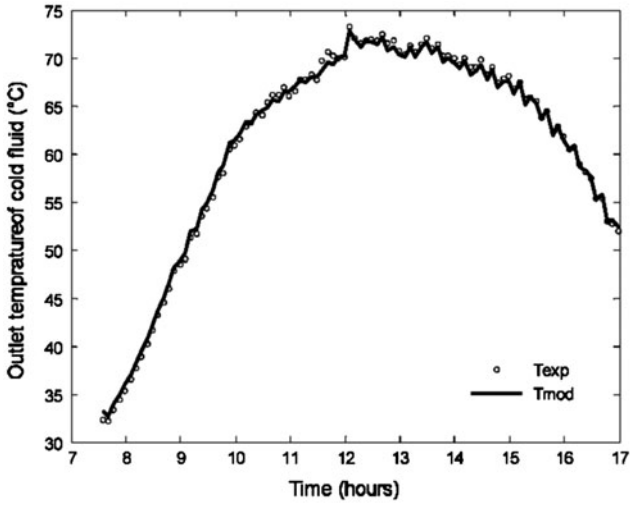

Fig. 6. Temperature profile for the theoretical and experimental cold fluid. Day: 9 June 2011, flow of coolant $\dot{m}_{coolant} = 770\,kg/h$, flow of cold fluid $\dot{m}_{feed} = 1{,}200\,kg/h$.

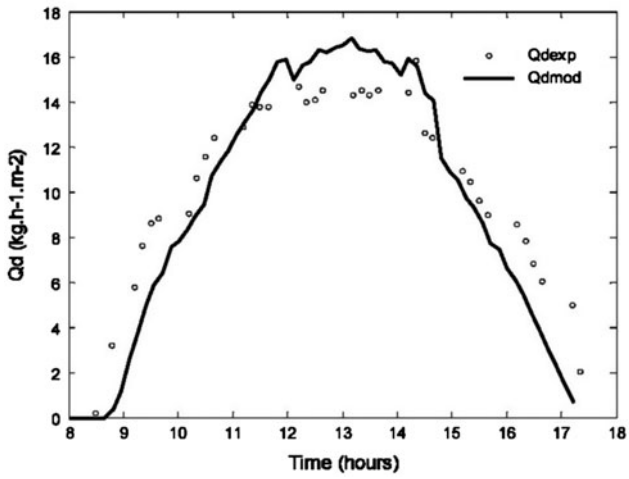

Fig. 7. Variation of distillate flux against time Day: 9 June 2011, $\dot{m}_{coolant} = 770\,kg/h$, $\dot{m}_{feed} = 1{,}200\,kg/h$.

A system for regulating the inlet temperature is crucial for the protection of the membrane. Such a system will be used to control the flow rate of seawater supplementary and the retentate flow rate rejected.

Regarding the heat exchanger, the difference is about 3.2% for the temperatures of hot fluid and does not exceed 1% for the cold fluid temperatures.

Fig. 7 shows an example of comparison between the variations of distillate flow rate determined experimentally and calculated by the model. The simulation results are obtained using as input the real data measured experimentally. These data are the water temperature at the inlet of the module, the feed flow rate, and the vacuum pressure.

Experimentally, it is very difficult to maintain a constant vacuum pressure along the manipulation, indeed the pressure varies between 10,000 and 15,000 Pa. Fluctuations in the vacuum pressure have led to a not smooth profile of the permeate flow rate. The quantity of permeate produced depends on the temperature of the fluid feeding the membrane (Eq. (22)). Indeed, the increase in the temperature allows, on the one hand, to improve the permeability (Eq. (16)) and secondly, to increase the pressure gradient on either side of the membrane (Eqs. (17) and (18)). The temperature of seawater at the inlet of membrane evolves along the time following the solar flux. The production begins when the required level of temperature is reached and also follows the evolution of the solar flux. Maximum permeate flow rates are obtained in the middle of the day: this is the period for which we have the maximum radiation levels and, therefore, the highest temperature at the inlet of the membrane module.

For all manipulations performed, the difference between the flow rate of distillate obtained experimentally and that estimated by the model is about 15%. These relatively large differences between the experiment and simulation are due to disturbances in the vacuum pressure applied. On the other hand, this difference can be justified by the change in permeability during the manipulation to the accumulation of salt on the membrane surface, something that affects the porosity of the membrane. The Knudsen permeability of the membrane at 20°C is $1.92 \times 10^{-6}\,s\,mol^{0.5}\,kg^{-0,5}\,m^{-1}$ which corresponds to $k_{m0} = 1.505 \times 10^{-8}\,s\,m^{-1}\,K^{-0,5}$.

4.2. Simulation of the operation of the installation

The global model is established by taking into account the accumulation of matter and heat in the tank. It is assumed that the condensation is complete.

4.2.1. Estimation the solar flux

The density of solar radiation received by the collector field varies during the day according to a sinusoidal law [17]:

$$E(t) = E_{max} \sin\left(\pi \frac{t - t_{sunrise}}{t_{sunset} - t_{sunrise}}\right) \quad (28)$$

E_{max}, maximum solar flux received by the collector during the day; $t_{sunrise}$, time corresponding to sunrise for a given day; t_{sunset}, time corresponding to sunset for a given day.

Four typical days representing the four seasons of the year were chosen: the equinoxes (21 March and 21 September) and solstices (21 June and 21 December). Fig. 8 shows the variation of solar flux for the four typical days of the year according to time.

4.2.2. *Influence of the vacuum pressure, the feed flow rate, and the inlet temperature*

The global model developed allowed us to perform a parametric study that quantifies the influence of different parameters. This study was useful in selecting appropriate operating conditions. Among the studied parameters, we include the influence of coolant flow rate, the feed flow rate, and the level of vacuum applied.

For example, Fig. 9 shows the effect of the vacuum pressure applied to the flow rate of distillate collected. It follows from the analysis of these curves that the distillate flow rate gradually increases at the beginning of the day, reaches its maximum around midday, and decreases gradually toward the sunset: it, therefore, follows the solar flux. The permeate flow rate increases with the increase of the pressure gradient which is the driving force of the transfer. Work with reduced pressures allows the evaporation of seawater for relatively low temperatures; this makes us increase the duration of production and especially earn in terms of daily production. Indeed, production passes from 48.6 kg at a vacuum pressure of 20,000 Pa to 116.5 kg at a pressure of 5,000 Pa.

Fig. 10 shows the evolution of the distillate flow rate as a function of feed flow rate. These curves show that the flow rate of distillate is influenced by varying the feed flow rate. Distillate flux vary from 81 to 98 kg/h/m^2 for the feed rates 600 and 2,400 kg/h, which represents a gain of 21% of daily production. This increase is due to the improvement of the transfer of heat and mass in the membrane following the increase of the flow rate of seawater

The feed flow rate must be sufficient to limit membrane fouling (v_{feed}>0.5 m s^{-1}). On the other hand, the choice of an optimal flow rate must result from a technical and economic study taking into account the cost of pumping and the influence of flow increases about the longevity of membranes.

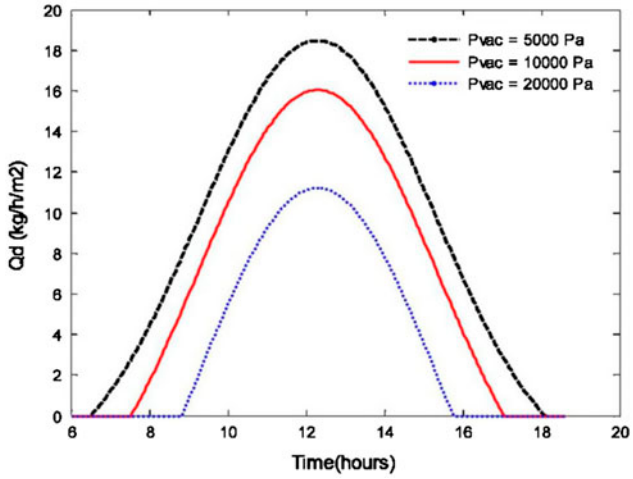

Fig. 9. Variation of the distillate flow rate according to the vacuum pressure. $\dot{m}_{feed}$ = 1,200 kg/h, $\dot{m}_{coolant}$ = 770 kg/h, Day: 21 March.

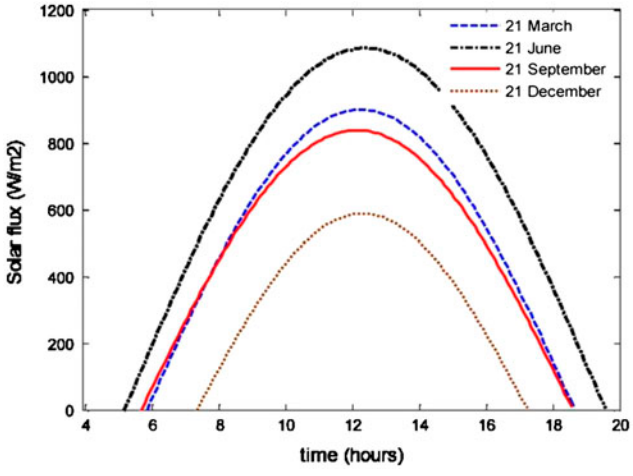

Fig. 8. Evolution of the solar flux based on a typical year days.

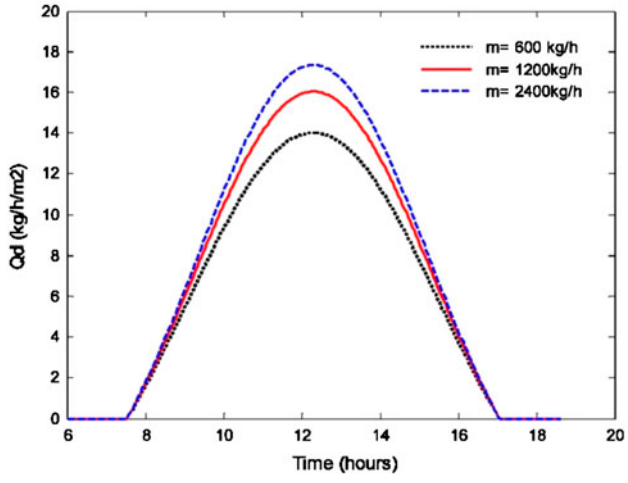

Fig. 10. Variation of the distillate flow rate according to the feed flow. P_{vacuum} = 10,000 Pa, $\dot{m}_{coolant}$ = 770 kg/h, Day: 21 March.

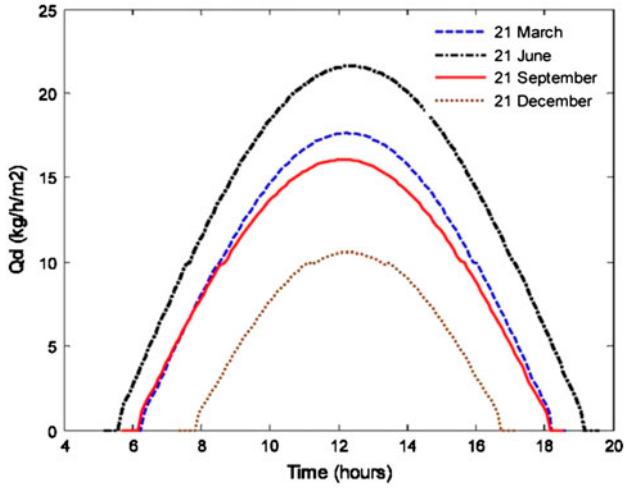

Fig. 11. Variation of the simulated flow rate of distillate vs. time for different year days. $P_{vacuum} = 5{,}000\,Pa$, $\dot{m}_{coolant} = 770\,kg/h$, $\dot{m}_{feed} = 1{,}200\,kg/h$.

4.2.3. Estimation of productivity

The model describing the functioning of the collector field allows estimating the evolution of the temperature of the coolant during the day. The model describing the functioning of the plate heat exchanger is used to determine the temperature of the water feeding the membrane. The model describing the behavior of hollow fiber membrane module was used to evaluate, instantly and at each position, the steam and retentate temperatures and the flow rate of distillate and estimate the daily production. As an example, Fig. 11 presents the instantaneous variation of desalinated water production for the four typical days of the year. The flow rate of the distillate gradually increases at the beginning of the day and it decreases gradually at the end of the day. Therefore, the production reaches its maximum value for 21 June, it is around $22\,kg\,h^{-1}\,m^{-2}$. The production is almost the same for both days of the equinox; it is about $17\,kg\,h^{-1}\,m^{-2}$. For the 21 December (winter day), production is $10\,kg\,h^{-1}\,m^{-2}$. Production varies in a remarkable manner throughout the day due to the variation of solar flux. The daily productivity is between 63 and $188\,kg\,m^{-2}$ for the days of 21 December and 21 June; this corresponds to average flow rates from 8 to $14\,kg\,h^{-1}\,m^{-2}$ on the basis of the sunny period of the day.

5. Conclusion

To develop a model describing the functioning of the desalination plant membrane coupled with solar energy, we developed three models for the three essential components of the system: the field of solar collectors, the membrane module, and the plate heat exchanger. The models are based on balance equations of mass and heat under transient conditions on the three organs. The comparison of experimental tests with those from the model showed the validity of the established models. The largest differences are observed for the model describing the functioning of the membrane module. Variations in levels of vacuum applied during manipulation and fluctuations of the solar flux are the main source of these differences.

From these models, we developed calculation programs on the software MATLAB and this in order to simulate and study the functioning of the unit. The models developed are able to determine the evolution of temperatures at each organ in any position and over time and changes the flow rate of distillate during the day. The model allows studying the influence of various operating parameters such as flow rate of feed, coolant flow rate, etc. The study shows that the applied vacuum pressure is a key parameter; very extensive levels of vacuum pressure can increase considerably the flow rate of distillate product.

This model determines the performance of the unit over time and for any day of the year. Simulations proved that pilot plant is able to provide average permeate flow rate ranging from $8\,kg\,h^{-1}\,m^{-2}$ for 21 December to $14\,kg\,h^{-1}\,m^{-2}$ for 21 June.

The models developed are very useful for controlling and regulating the installation. A system for regulating the inlet temperature of the membrane module is highly recommended for the maximum temperature that can support the membrane (75°C).

The prospects consist essentially in determining the optimal operating conditions and to carry a energetic study of the pilot. These conditions concern mainly the flow rate of coolant and its regulation as a function of solar radiation, the flow rate of seawater, and the rejection rate of the retentate.

Symbols

C_p	—	heat capacity ($J\,kg^{-1}\,C^{-1}$)
d	—	diameter (m)
E	—	solar flux density ($W\,m^{-2}$)
e	—	thickness of the absorber plate (m)
h	—	heat transfer coefficient ($W\,m^{-2}\,C^{-1}$)
J_v	—	flux density of water ($kg\,m^{-2}\,s^{-1}$)
k_m	—	Knudsen permeability ($s\,m^{-1}$)
L_v	—	latent heat of vaporization ($J\,kg^{-1}$)
l_A	—	width of the absorber plate (m)
$\dot{m}$	—	mass flow rate ($kg\,h^{-1}$)

n_{fib} — fiber number (−)
n_t — total number of points (−)
P — pressure (Pa)
Q_v — flow rate ($m^3 h^{-1}$)
S — area (m^2)
T — temperature (°C)
t — time (s)
U — overall heat transfer coefficient ($W m^{-2} K^{-1}$)
v — velocity ($m s^{-1}$)
z — distance (m)

Greek symbols

α — absorbance of collector (−)
ρ — density ($kg^{-1} m^{-3}$)
τ — emissivity of collector (−)

Subscripts

Ab — absorber
amb — ambient
C — cold fluid
dist — distillate
exp — experimental
ex — external
Fd — coolant
fib — fibre
H — hot fluid
in — internal
mod — model
ref — reference
vac — vacuum
W — wall

Acknowledgment

The authors address their thanks to the European Commission for funding the cooperation project FP6 Membrane-Based Desalination: An Integrated Approach. MEDINA Project No: 036997.

References

[1] F. Trieb, H. Steinhagen, Concentrating solar power for seawater desalination in the Middle East and North Africa, Desalination 220 (2008) 165–183.
[2] F. Ben Jemaa, I. Houcine, M.H. Chahbani, Desalination in Tunisia: Past experience and future prospects, Desalination 116 (1998) 123–134.
[3] S. Bouguecha, B. Hamrouni, M. Dhahbi, Small scale desalination pilots powered by renewable energy sources: Case studies, Desalination 183 (2005) 151–165.
[4] M.R. Qtaishat, F. Banat, Desalination by solar powered membrane distillation systems, Desalination 308 (2013) 186–197.
[5] J.P. Mericq, S. Laborie, C. Cabassud, Vacuum membrane distillation for an integrated seawater desalination process, Desalin. Water Treat. 9 (2009) 293–302.
[6] E. Mathioulakis, V. Belessiotis, E. Delyannis, Desalination by using alternative energy: Review and state-of-the-art, Desalination 203 (2007) 346–365.
[7] F. Banat, N. Jwaied, Economic evaluation of desalination by small-scale autonomous solar-powered membrane distillation units, Desalination 220 (2008) 566–573.
[8] A. Zrelli, B. Chaouchi, S. Gabsi, Simulation of vacuum membrane distillation coupled with solar energy: Optimization of the geometric configuration of a helically coiled fiber, Desalin. Water Treat. 36 (2011) 41–49.
[9] J.-B. Gálveza, L. García-Rodríguezb, I. Martín-Mateosclination, Seawater desalination by an innovative solar-powered membrane distillation system: the MEDESOL project, Desalination 246 (2009) 567–576.
[10] N. Frikha, B. Chaouachi, S. Gabsi, Design of a semi industrial scale pilot for sea water desalination with a solar membrane distillation, MEDINA EU-China, Qingdao, p. 10 2009.
[11] N. Frikha, R. Matlaya, B. Chaouachi, S. Gabsi, Conception d'une installation de distillation membranaire sous vide de l'eau de mer fonctionnant totalement à l'énergie solaire [Design of a pilot of vacuum membrane distillation for seawater functioning completely with solar energy]. Récents Progrès en Génie des Procédés, Lille, 2011.
[12] H. Benbacha, M. Baccar, A. Maalej, Dynamic modelling and simulation of a new air conditioning prototype by solar energy, Renewable Energy 32 (2007) 200–215.
[13] V. Calabrol, E. Driolil, Polarization phenomena in integrated reverse osmosis and membrane distillation for seawater desalination and waste water treatment, Desalination 108 (1996) 81–82.
[14] C. Cabassud, D. Wirth, Membrane distillation for water desalination: How to chose an appropriate membrane? Desalination 157 (2003) 307–314.
[15] D. Wirth, C. Cabassud, Water desalination using membrane distillation: Comparison between inside/out and outside/in permeation, Desalination 147 (2002) 139–145.
[16] B. Li, K.K. Sirkar, Novel membrane and device for vacuum membrane distillation-based desalination process, J. Membr. Sci. 257 (2005) 60–75.
[17] J.-P. Mericq, S. Laborie, C. Cabassud, Evaluation of systems coupling vacuum membrane distillation and solar energy for seawater desalination, Chem. Eng. J. 166 (2011) 596–606.